

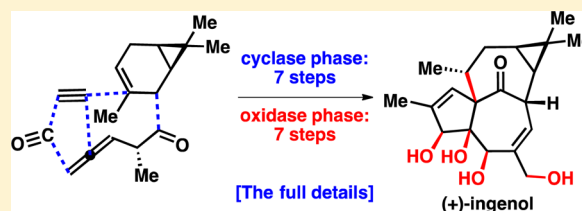
Development of a Concise Synthesis of (+)-Ingenol

Steven J. McKerrall, Lars Jørgensen,[†] Christian A. Kuttruff,[†] Felix Ungeheuer, and Phil S. Baran*

Department of Chemistry, The Scripps Research Institute, 10550 North Torrey Pines Road, La Jolla, California 92037, United States

S Supporting Information

ABSTRACT: The complex diterpenoid (+)-ingenol possesses a uniquely challenging scaffold and constitutes the core of a recently approved anti-cancer drug. This full account details the development of a short synthesis of **1** that takes place in two separate phases (cyclase and oxidase) as loosely modeled after terpene biosynthesis. Initial model studies establishing the viability of a Pauson–Khand approach to building up the carbon framework are recounted. Extensive studies that led to the development of a 7-step cyclase phase to transform (+)-3-carene into a suitable tigliane-type core are also presented. A variety of competitive pinacol rearrangements and cyclization reactions were overcome to develop a 7-step oxidase phase producing (+)-ingenol. The pivotal pinacol rearrangement is further examined through DFT calculations, and implications for the biosynthesis of (+)-ingenol are discussed.



INTRODUCTION

For decades, architecturally complex terpenoid natural products have pushed the limits of both the strategies and methods employed in organic synthesis. As one of the most diverse classes of secondary metabolites, terpenes continue to provide significant challenges through their extensive oxidation and varied, unique skeletons.¹ Terpenes have historically driven improvements in the synthesis of polycyclic molecules,² fostered the development of retrosynthetic analysis,³ and led to numerous broadly useful methods for the formation of carbon–carbon bonds.⁴ In addition, the important biological function and use of terpenoids in medicines necessitate improved routes for their preparation and for the development of more medicinally valuable analogues.⁵ This full account traces the development of a concise total synthesis of the complex terpenoid (+)-ingenol (**1**, Figure 1).⁶

The *Euphorbia* genus of plants contains a variety of heavily oxidized diterpenoid natural products.⁷ Among the most notable members of this family of natural products is the diterpenoid ingenol (**1**). Ingenol (**1**) was isolated in 1966 by Hecker and co-workers from *Euphorbia ingens*, from which its name is derived.⁸ **1** was initially isolated on the basis of irritant activity, and its structure was not elucidated until 1967, when an X-ray crystal structure of the triacetate was obtained.⁹ The structure of **1** contains a number of challenging features found in many oxidized terpene natural products, including a congested stereogenic triol moiety, a neighboring all-carbon quaternary stereocenter, and a dimethylcyclopropane. Unique to **1**, however, is the bicyclo[4.4.1]undecane core bearing a *trans*-intra-bridgehead stereochemical configuration, also known as *in/out* stereochemistry.^{10,11} The configuration of the bridgehead hydrogen imparts significant angular strain on the bicyclic framework, as evidenced by the substantially elongated bond angles found in the X-ray crystal structure obtained for 20-deoxyingenol (**2**).

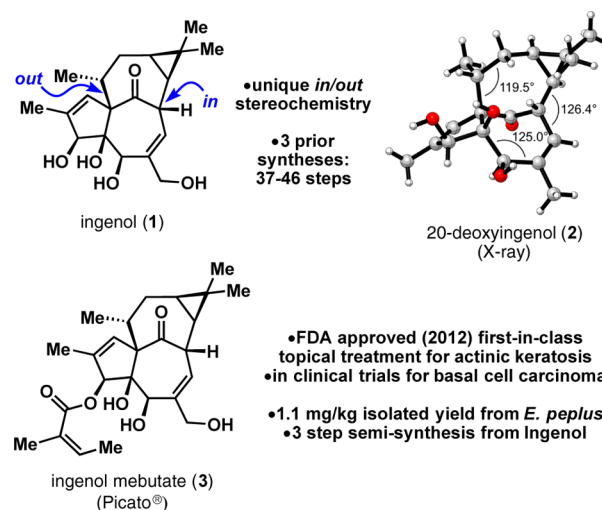


Figure 1. Diterpenoids ingenol (**1**), 20-deoxyingenol (**2**), and ingenol mebutate (**3**).

In addition to their structural complexity, ingenane diterpenes possess important biological activity. Derivatives of **1** are reported to possess activity ranging from anti-cancer^{12a} to anti-HIV;^{12b} however, the most medicinally important derivative of **1** is ingenol mebutate (**3**), commercially available as Picato, developed by LEO Pharma. Ingenol mebutate (**3**) was approved by the FDA in early 2012 as a first-in-class topical treatment for actinic keratosis, a pre-cancerous skin condition.¹³ Isolated from *E. peplus*, **3** was discovered through a screen of medicinal plants used by indigenous populations in Australia.¹⁴ In addition to its FDA-approved indications, **3** has undergone

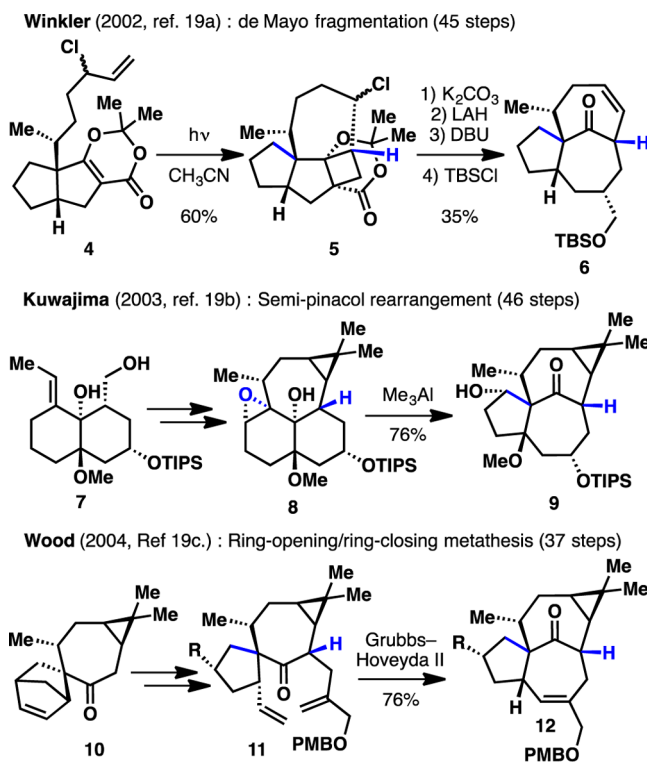
Received: February 26, 2014

Published: April 8, 2014

clinical testing for the topical treatment of both basal cell carcinoma and squamous cell carcinoma.¹⁵ Interestingly, the mechanism of action is not well understood. A dual-phase mechanism has been proposed consisting of an initial ill-defined necrotic cell-killing mechanism, followed by immune stimulation mediated by activation of protein kinase C, ultimately leading to apoptosis.¹⁶ Currently, **3** is obtained by a tedious isolation protocol, in a low yield of ~1.1 mg/kg.¹⁷ A semisynthesis of **3** has also been developed from ingenol (**1**), which can be isolated in a greater yield of ~250 mg/kg.¹⁸ While these methods have proved capable of delivering the necessary quantities for clinical testing and development, the isolation procedures are inefficient, difficult, and costly. In addition, a bioengineering approach is severely hampered by the poorly understood, complex biosynthesis described below. Most importantly, from the perspective of developing new medicines, available semisynthetic modifications of **1** are limited, and a rigorous structure–activity relationship has remained elusive. These challenges led LEO Pharma to initiate a collaboration with our laboratory with the aim of developing a blueprint for the chemical synthesis of **1** that would be amenable to large-scale preparation.

The unusual structural features of ingenol (**1**), combined with its biological promise, have motivated significant interest from synthetic chemists. Several decades of effort culminated in three total syntheses of **1** (Scheme 1),¹⁹ one total synthesis of

Scheme 1. Previous Approaches to the Total Synthesis of Ingenol (**1**)



13-oxyingenol,²⁰ and numerous approaches to the tricyclic skeleton.²¹ Each of these syntheses is a landmark achievement, but they require a large number of chemical manipulations (37–46 steps) to prepare **1**. In order to access fully synthetic analogues of ingenol mebutate (**3**), we also required an approach that would be amenable to late-stage diversification.

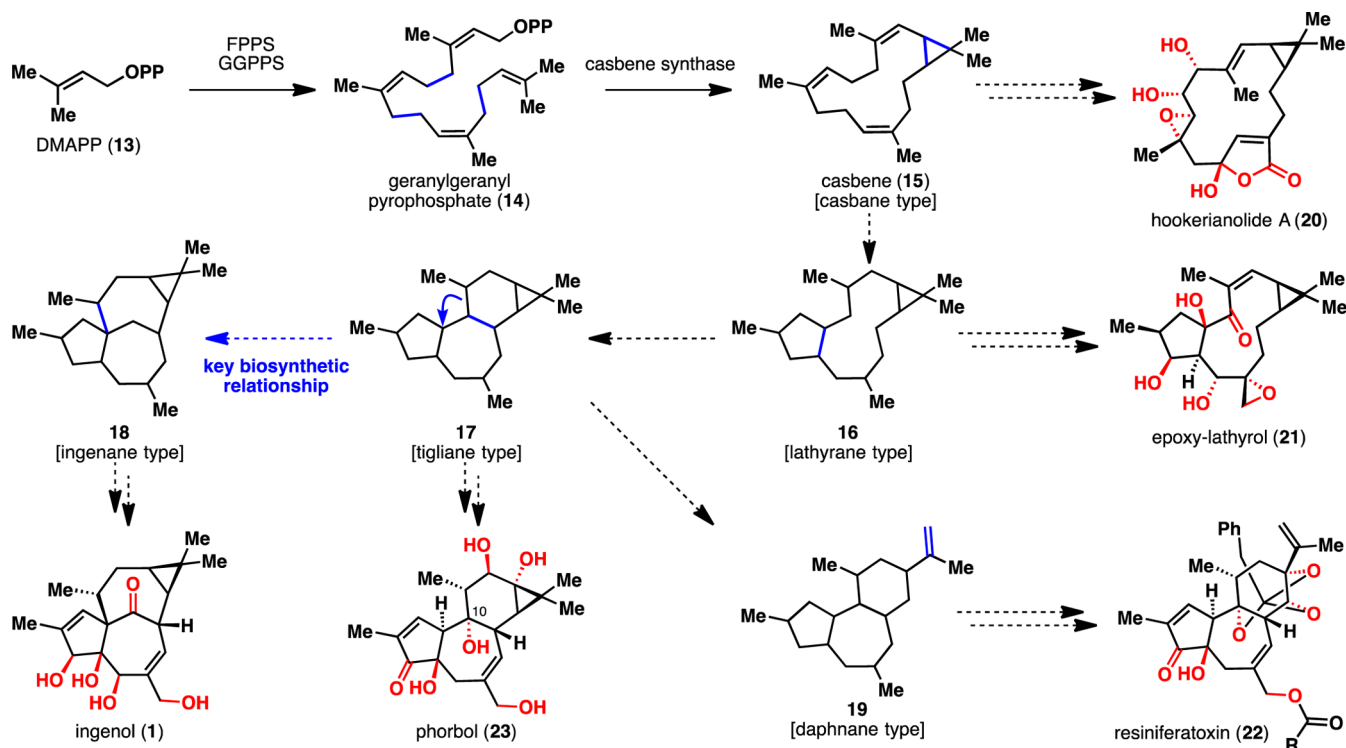
To this end, an expedient synthesis was sought that would be amenable to both the preparation of large quantities of **1** and the diversion of a late-stage intermediate to novel analogues of **3**.²²

Our insights into the retrosynthetic analysis of **1** were greatly influenced by the biosynthesis of *Euphorbia* diterpenes (Scheme 2). The biosynthesis is thought to begin with the formation of casbene (**15**) and continue with stepwise cyclizations to form the carbon skeletons of the lathyrane (**16**), tigliane (**17**), ingenane (**18**), and daphnane (**19**) natural products.^{7,23} It should be noted that only the biogenesis of casbene (**15**) has been characterized in any detail, and subsequent biosynthetic steps are speculative.²⁴ The proposal of intermediate cyclizations is best supported by the existence of oxidized natural products (**20–23**) with each of the intermediate scaffolds. The level of oxidation that is installed during the various cyclase steps also remains a mystery, and it is likely that some cyclase and oxidase steps intertwine in the biosynthesis of *Euphorbia* diterpenes. Nevertheless, the general wisdom of first forming an unfunctionalized carbon skeleton and then diversifying to various molecules through oxidation and rearrangement is preserved.

RESULTS AND DISCUSSION

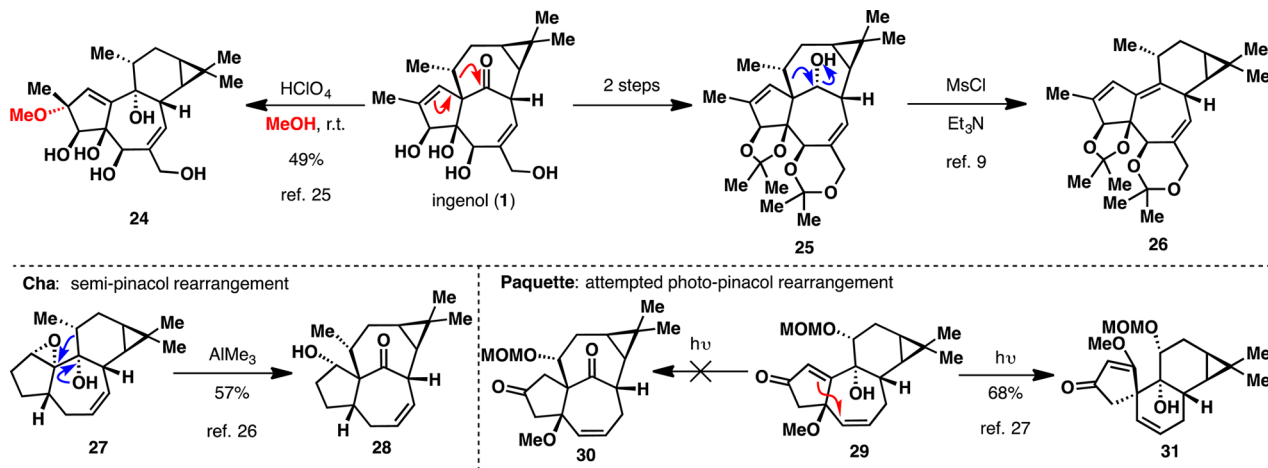
Retrosynthetic Analysis. Our retrosynthetic analysis began with the realization that the biosynthetic step connecting the tigliane (**17**) and ingenane (**18**) skeletons was a greatly simplifying disconnection. The rearrangement of **17** to **18** forms the all-carbon quaternary stereocenter, installs the bicyclic skeleton, and secures the *in/out* stereochemistry. While the biosynthesis of **1** remains largely speculative, the rearrangement is likely a pinacol-type 1,2 migration since tigliane natural products generally contain the necessary tertiary alcohol seen in phorbol (**23**, C-10). Furthermore, application of the isoprene rule to **1** indicates a structural rearrangement.⁷ In further support of this connection, a retro-pinacol rearrangement of **1** has been observed under mild conditions to give tigliane-type compound **24** (Scheme 3).²⁵ Additionally, activation of the secondary alcohol in **25** leads to a similar 1,2-shift to give **26**.⁹ In the forward direction, Cha has shown that epoxy-alcohol **27** rearranges to **28** upon treatment with AlMe_3 to form the carbocyclic skeleton of **1**.²⁶ Paquette also attempted a photo-pinacol rearrangement of **29**, but those efforts were thwarted by competitive rearrangements to give products such as **31** instead.²⁷ The formation of **24** from **1** supports the biosynthetic relationship but was troubling from our vantage point because it implies that the pinacol rearrangement is energetically unfavorable and a tigliane skeleton (**24**, **26**) is the thermodynamically favored ring system. In the case of **27**, the epoxide strain compensates for the *in/out* bicycle, but in our design there is no such driving force. Despite these clear challenges, we viewed the disconnection as powerfully simplifying and designed our synthesis around a biomimetic vinylogous pinacol rearrangement linking the tigliane ring system to the ingenane ring system.

In addition to mimicking a biosynthetic reaction to form the *in/out* stereochemistry, we also sought to borrow the general two-phase strategy that nature employs in terpenoid biosynthesis.²⁸ In this design, abiotic carbon–carbon bond-forming reactions would deliver a key carbon skeleton, and subsequent substrate-controlled oxidation and rearrangement would deliver **1**. Thus, **1** would be formed from **32**, bearing minimal oxidation

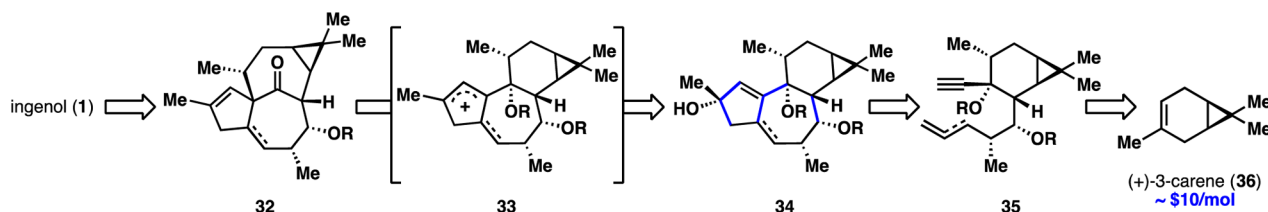
Scheme 2. Unified Biosynthesis of *Euphorbia* Diterpenoids^a

^aAbbreviations: DMAPP = dimethylallyl pyrophosphate, FPPS = farnesyl pyrophosphate synthase, GGPPS = geranyl geranyl pyrophosphate synthase.

Scheme 3. Pinacol and Retropinacol Rearrangements in the Ingenane Scaffold

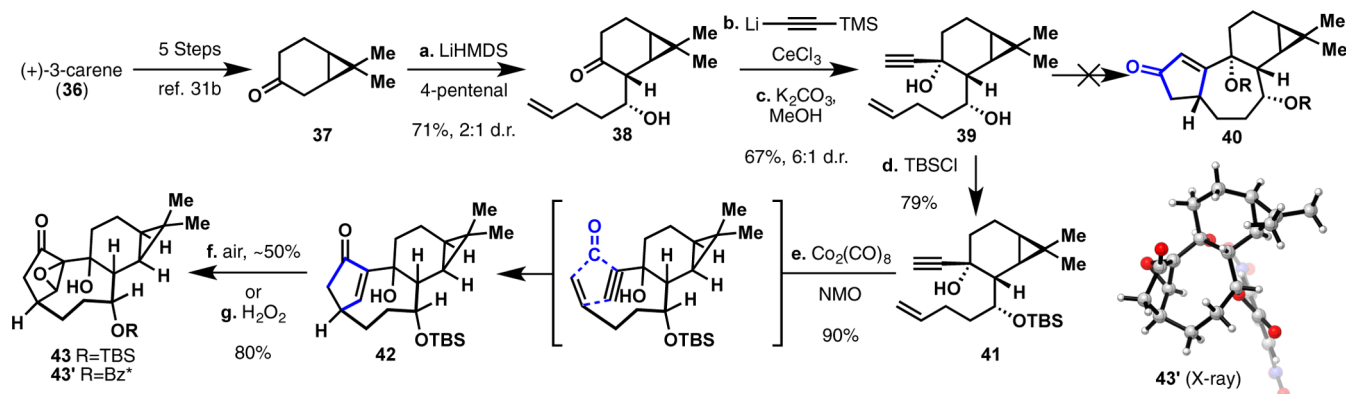


Scheme 4. Retrosynthetic Analysis of Ingenol (1)



(Scheme 4). Ingenane **32** would be formed by a vinylogous pinacol rearrangement, via carbocation **33**, from tiglane core **34**. The tiglane skeleton in **34** would be secured through a Pauson–Khand (P-K) cyclization²⁹ of **35**, which would in turn

be derived from inexpensive (+)-3-carene (**36**).³⁰ In addition to producing **1**, this route would be amenable to late-stage diversification of the key hydroxyl groups to form novel synthetic analogues of ingenol mebutate (**3**).

Scheme 5. Synthesis and Evaluation of Ene-yne Pauson–Khand Model Compounds^a

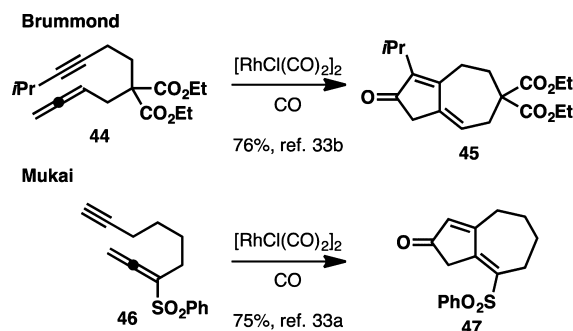
^aReagents and conditions: (a) LiHMDS, 4-pentenal, THF, $-78\text{ }^{\circ}\text{C}$, 71%, 2:1 dr; (b) TMS-acetylene, *n*-BuLi, CeCl_3 , THF, $-78\text{ }^{\circ}\text{C}$; (c) K_2CO_3 , MeOH, rt, 67% over 2 steps, 6:1 dr; (d) TBSCl, imidazole, DMF, $60\text{ }^{\circ}\text{C}$, 79%; (e) $\text{Co}_2(\text{CO})_8$ (1.0 equiv), NMO, CH_2Cl_2 , $0\text{ }^{\circ}\text{C}$ to rt, 90%; (f) air, CHCl_3 , rt, $\sim 50\%$; (g) H_2O_2 , NaOH, MeOH, rt, 80%. Abbreviations: LiHMDS = lithium hexamethyldisilazide, THF = tetrahydrofuran, TBSCl = *tert*-butyldimethylsilyl chloride, DMF = *N,N*-dimethylformamide, NMO = *N*-methylmorpholine *N*-oxide, Bz* = 2,4-dinitrobenzoate.

Model Pauson–Khand Studies. In order to quickly establish the viability of a P-K approach to tigliane-type compound **34**, studies began on a more easily accessible model system lacking the C-ring methyl group. Whereas no routes were known at the time to the requisite methyl ketone (**SI-6**), ketone **37** could be easily prepared from (+)-3-carene (**36**) according to literature procedures (Scheme 5).^{31b} Kinetic deprotonation of **37** with LiHMDS followed by treatment with 4-pentenal gave aldol adduct **38** in 71% yield and a 2:1 mixture of alcohol epimers. Acetylide addition was accomplished in 2 steps using the TMS-protected cerium acetylide followed by deprotection with K_2CO_3 and MeOH to give diol **39** in 67% yield as a 6:1 mixture of diastereomers. Unfortunately, cyclization of **39**, or a variety of protected derivatives, failed to deliver **40** under several conditions attempted. In general, no reaction was observed, followed by eventual decomposition.

The single exception, TBS-protected substrate **41**—formed by treatment of **39** with TBSCl in 79% yield—was reactive under classical P-K conditions. Thus, treatment of **41** with stoichiometric $\text{Co}_2(\text{CO})_8$, followed by NMO, produced an unusual enone **42** which contains a *trans* 8-membered ring. This product presumably arises from a head-to-tail reaction of the alkene and alkyne rather than the typically observed head-to-head reaction. In contrast, diol **39** or a variety of related derivatives simply underwent decomplexation upon treatment of the *in situ* formed cobalt–alkyne complex with NMO. Although this reactivity has been reported previously, the origin of this selectivity remains unknown.³² Enone **42** was readily auto-oxidized in the presence of air and light to produce epoxide **43**, and an X-ray crystal structure of derivative **43'** confirmed the unusual ring system and the initial head-to-tail reaction by inference.

The failure of **39** to undergo the desired ene-yne P-K cyclization led us to reconsider our strategy to the tigliane ring system in **34**. Several variants of the P-K reaction have been detailed.²⁹ In particular, reports from the Brummond and Mukai laboratories detailing rhodium-catalyzed allene-yne P-K reactions (Scheme 6) were extremely promising because they showed examples in which 7- and even 8-membered rings could be formed in good yield.³³ Motivated by these reports, we revised our strategy to target an allene-yne intermediate. In addition to aiding in the formation of the central 7-membered

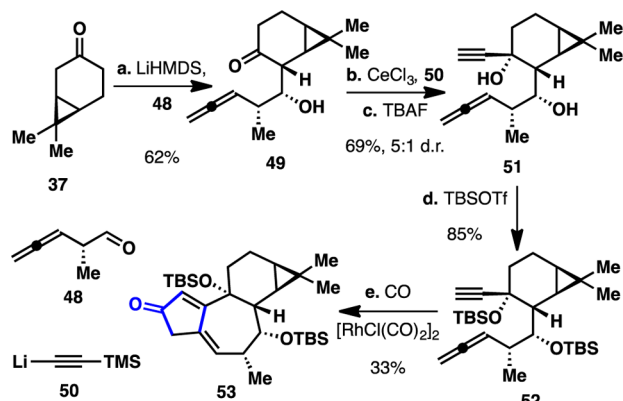
Scheme 6. Previous Examples of Allene-yne Pauson–Khand Cyclizations



ring, this subtle change would also install an additional olefin in the cyclase phase product, which could be more easily transformed to the requisite diol than a saturated counterpart.

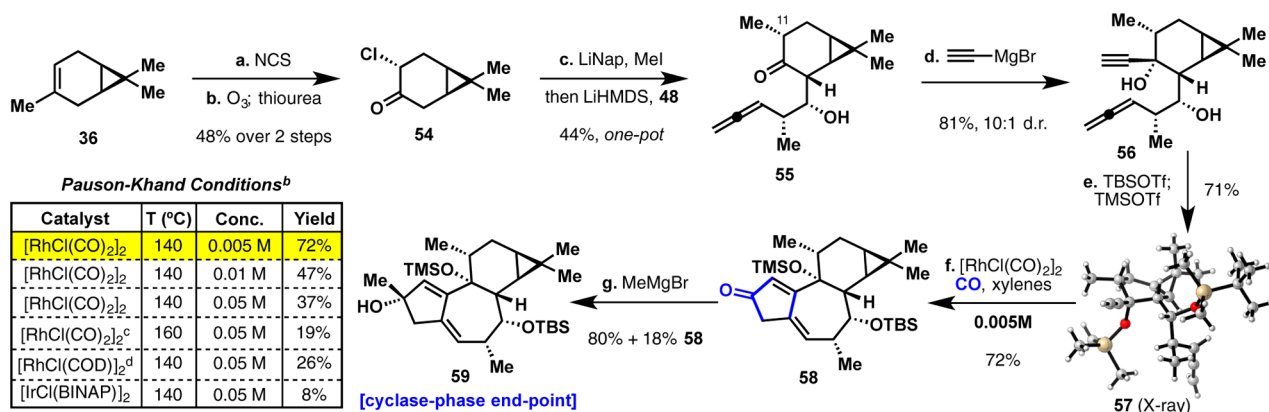
The synthesis of the allene-yne model system again begins with ketone **37**, which was deprotonated with LiHMDS then treated with chiral aldehyde **48** to provide adduct **49** in 62% yield as a single observable diastereomer (Scheme 7). Two-step ethynylation using the organocerium reagent derived from **50** and deprotection provided diol **51** in 69% yield as a 5:1 mixture of diastereomers. Whereas diol **51** decomposed quickly under standard P-K conditions, the bis-TBS-protected substrate **52** successfully underwent cyclization upon treatment with catalytic quantities of $[\text{RhCl}(\text{CO})_2]_2$ under a CO atmosphere to give dienone **53** in 33% yield as the only observed regioisomer. With this result in hand, it was clear that an allene-yne P-K reaction could, in principle, deliver the key precursor to ingenol (**1**).

Cyclase Phase. With a proof of concept for constructing a viable tigliane precursor, the next challenge encountered was installation of the missing C-11 methyl group.³¹ To this end, it was discovered that (+)-3-carene (**36**) could be regioselectively chlorinated with NCS and catalytic DMAP (Scheme 8). Subsequent ozonolysis of the exocyclic olefin delivered **54** in 48% yield over 2 steps. The requisite methyl ketone (**SI-6**) could be synthesized as a single diastereomer by treatment with lithium naphthalenide (LiNap) followed by methyl iodide; however, it was discovered that isolation of the methyl ketone was operationally challenging. Gratifyingly, sequential treat-

Scheme 7. Successful Allene-yne Model System^a

^aReagents and conditions: (a) LiHMDS, **48**, THF, $-78\text{ }^{\circ}\text{C}$, 62%; (b) TMS-acetylene, *n*-BuLi, CeCl_3 , THF, $-78\text{ }^{\circ}\text{C}$; (c) TBAF, THF, $0\text{ }^{\circ}\text{C}$, 69% over 2 steps, 5:1 d.r.; (d) TBSOTf, Et_3N , CH_2Cl_2 , $0\text{ }^{\circ}\text{C}$ to rt, 85%; (e) $[\text{RhCl}(\text{CO})_2]_2$ (0.1 equiv), CO, PhMe, $110\text{ }^{\circ}\text{C}$, 33%. Abbreviations: TBAF = tetrabutylammonium fluoride, TBSOTf = *tert*-butyldimethylsilyl triflate.

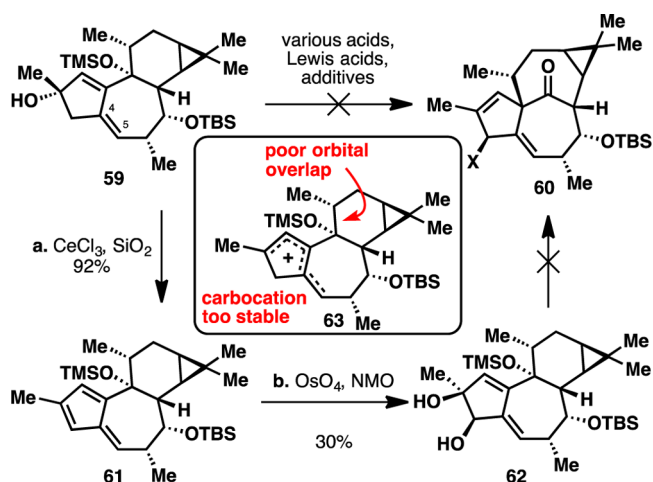
ment of chloroketone **54** with LiNap and MeI, followed by the addition of LiHMDS and aldehyde **48**, delivered aldol product **55** as a single diastereomer in 44% yield in a one-pot operation. Ethynylation was accomplished by treatment with ethynylmagnesium bromide to provide **56** in 81% yield as a 10:1 mixture of diastereomers. One-pot protection by successive treatment with TBSOTf then TMSOTf provided **57** in 71% yield. Bis-silyl ether **57** crystallized upon cooling, and X-ray crystallographic analysis confirmed the stereochemistry of the four stereocenters formed in the sequence. P-K cyclization with catalytic $[\text{RhCl}(\text{CO})_2]_2$ under CO atmosphere at 0.005 M concentration delivered dienone **58** in 72% yield. A summary of conditions examined is shown in Scheme 8. It was found that concentration has a dramatic impact on yield, with the yield improving from 37% to 72% upon a 10-fold dilution. Increased temperature and the use of other commonly employed catalysts provided inferior yields. Interestingly, iridium catalysis also

Scheme 8. Synthesis of Cyclase Phase End-Point **59**^a

^aReagents and conditions: (a) NCS, DMAP, CH_2Cl_2 , rt; (b) O_3 , CH_2Cl_2 , MeOH, $-78\text{ }^{\circ}\text{C}$, then thiourea, rt, 48% over 2 steps; (c) LiNap, MeI, HMPA, THF, $-78\text{ }^{\circ}\text{C}$, then LiHMDS, **48**, $-78\text{ }^{\circ}\text{C}$, 44%; (d) ethynylmagnesium bromide, THF, -78 to $0\text{ }^{\circ}\text{C}$, 81%, 10:1 d.r.; (e) TBSOTf, Et_3N , CH_2Cl_2 , $0\text{ }^{\circ}\text{C}$, then TMSOTf, Et_3N , 71%; (f) $[\text{RhCl}(\text{CO})_2]_2$ (0.1 equiv), CO, xylenes, $140\text{ }^{\circ}\text{C}$, 72%; (g) methylmagnesium bromide, THF, -78 to $0\text{ }^{\circ}\text{C}$, 80% + 18% **58**. ^bStandard conditions: catalyst (0.1 equiv), CO atmosphere, xylenes, temperature specified. ^cReaction conducted in 1,2-dichlorobenzene. ^dAdded dppp as a ligand. Abbreviations: NCS = *N*-chlorosuccinimide, DMAP = *N,N*-dimethylaminopyridine, HMPA = hexamethylphosphoramide, TMSOTf = trimethylsilyl triflate, dppp = 1,2-bis(diphenylphosphino)propane.

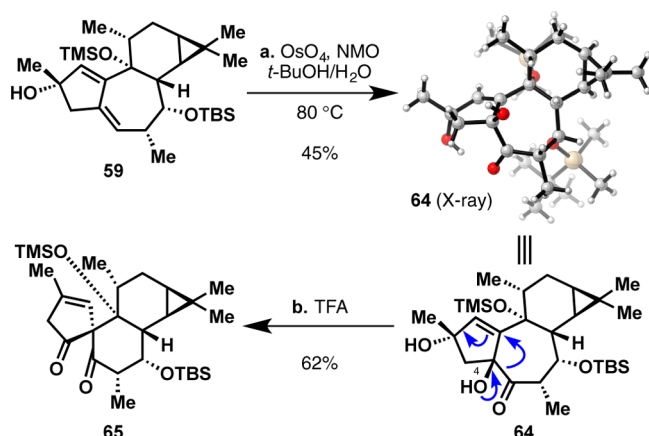
provided a small amount of product, but the yield could not be improved. The cyclase phase was completed by treatment of **58** with methylmagnesium bromide to provide **59** as a single diastereomer in 80% yield with 18% recovered **58**. With all of the carbon atoms in **1** installed in the form of precursor skeleton **59**, the core carbon skeleton was complete, and only oxidation and skeletal rearrangement remained.

Exploring the Pinacol Rearrangement. The first rearrangements targeted were directly on diene **59**. Despite many attempts, the desired rearrangement to **60** could not be accomplished (Scheme 9). It was found that under a variety of

Scheme 9. Attempted Pinacol Rearrangement of **59**^a

^aReagents and conditions: (a) CeCl_3 , SiO_2 , CH_2Cl_2 , rt, 92%; (b) OsO_4 (0.1 equiv), NMO, *t*-BuOH, H_2O , rt, 30%.

conditions for activating the tertiary alcohol, only elimination to form **61** was observed. Treatment of **59** with CeCl_3 and SiO_2 gave **61** in 92% yield. Fulvene **61** possesses oxidation in positions that could be useful for preparing **1**, so attempts were made to initiate the rearrangement from it. The fulvene in **61** could be dihydroxylated regioselectively using catalytic OsO_4 to

Scheme 10. Catalytic Dihydroxylation and Pinacol Rearrangement of **59**^a

^aReagents and conditions: (a) OsO₄ (0.1 equiv), NMO, *t*-BuOH, H₂O, 80 °C, 45%; (b) TFA, CH₂Cl₂, rt, 62%. TFA = trifluoroacetic acid.

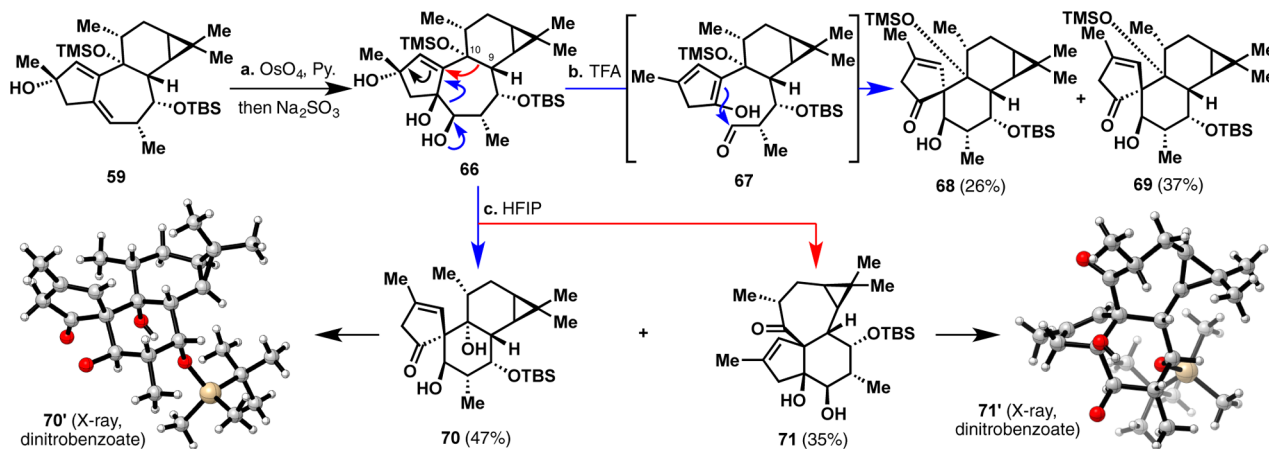
give **62** in 30% yield. Subsequent dihydroxylation failed under either catalytic or stoichiometric conditions. Again, attempted rearrangements of **62** to **60** were unsuccessful under a variety of conditions. Several explanations for the lack of desired reactivity can be made. For instance, the highly delocalized carbocation **63**—formed by ionization of **59**—could be too stable to give rise to the strained *in/out* bicycle. Alternatively, simple molecular modeling indicates that the presence of the diene forces the migrating bond to be nearly planar to the π -system and provides extremely poor orbital overlap for migration. Regardless of the explanation, it was reasoned that the C-4/C-5 olefin was severely limiting the desired reactivity, and removing it would provide a better opportunity to test the pinacol rearrangement.

Ultimately, the C-4/C-5 olefin in **59** needed to be converted to a 1,2-diol, so dihydroxylation of this substrate was attempted (Scheme 10). It was quickly found that the trisubstituted olefins in **59** were extremely hindered, and, under most typical conditions for OsO₄-catalyzed dihydroxylation, no turnover was

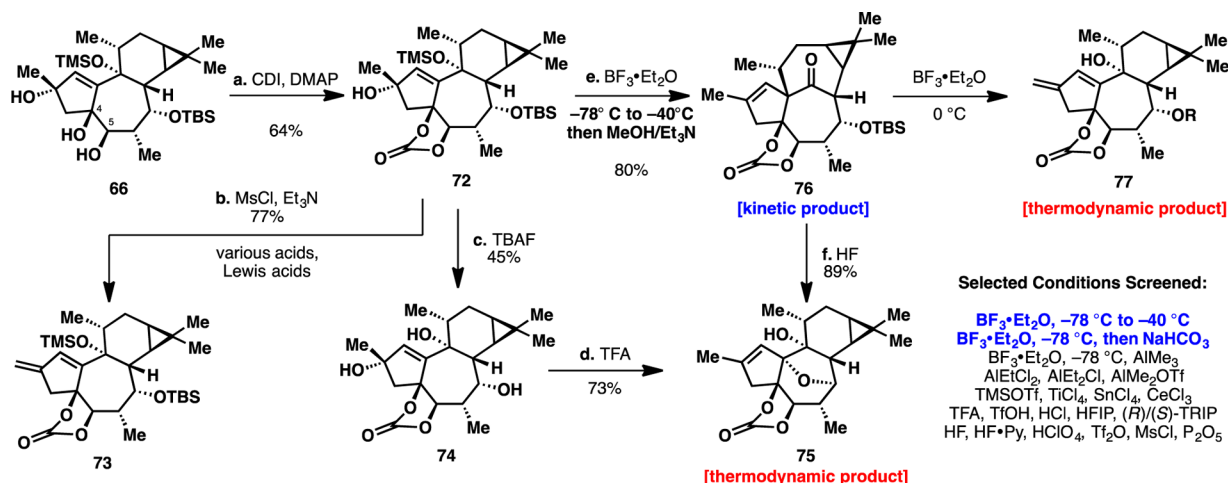
observed. Dihydroxylation conducted at high temperature produced ketol **64** in 45% yield instead of the desired diol. Surprisingly, even at partial conversion, only a mixture of ketol **64** and diene **59** was observed, implying that either the intermediate osmate decomposes to **64** directly or the over-oxidation is extremely rapid.³⁴ Reduction of the ketol **64** gave the undesired alcohol epimer, and activation of the tertiary alcohol with TFA produced spirocyclic diketone **65** in 62% yield as a single diastereomer. This product arises through a competitive pinacol rearrangement of the C-4 tertiary alcohol in **64**, which secures the observed stereochemical configuration of the newly formed quaternary carbon.

Successful dihydroxylation was ultimately achieved through a stoichiometric reaction with OsO₄ followed by reductive cleavage of the resulting osmate ester with Na₂SO₃ to deliver the diol **66** (Scheme 11). Treatment of **66** with TFA produces two major spirocyclic products, **68** and **69**—which differ only in the stereochemistry at the all-carbon quaternary stereocenter—in 26% and 37% yield from **59**, respectively. Spiro ketone **68** could potentially arise from a pinacol rearrangement reminiscent of the formation of **65**; however, the additional presence of the epimer at the quaternary stereocenter (**69**) suggests an alternative mechanism. The likely mechanism involves an initial Grob-type fragmentation to produce enol aldehyde **67**, followed by cyclization to produce a mixture of **68** and **69**. The use of numerous different conditions provided the same two products with only minor variations in the ratio. The single exception was found when heating **66** in HFIP produced epimeric spirocycle **70** and angularly fused **71** in 47% and 35% yield from **59**, respectively. Derivatization of **70** and **71** as dinitrobenzoates provided crystalline **70'** and **71'**, which allowed for X-ray crystallographic analysis to confirm the assigned structures. Spiro compound **70** likely arises through the same Grob-type fragmentation that produces **69**, while **71** arises from a direct rearrangement of **66** with migration of the undesired C-9/C-10 bond. The exact origin of **71** is unclear, but molecular modeling suggests that an unusual conformation of **66** is required for migration of the C-9/C-10 bond.

Spirocyclic rearrangements of diol **66** occur with the cleavage of the C-4/C-5 bond, so it was reasoned that a cyclic protecting group that is stable to acidic conditions would prevent

Scheme 11. Synthesis and Rearrangements of Diol **66**^a

^aReagents and conditions: (a) OsO₄ (1.0 equiv), pyridine, rt, then saturated aq Na₂SO₃, THF; (b) TFA, CH₂Cl₂, rt, 26% **68** + 37% **69**; (c) HFIP, 50 °C, 47% **70** + 35% **71**. HFIP = hexafluoroisopropanol. The dinitrobenzoate is omitted from the crystal structures shown for **70'** and **71'** for clarity. See Supporting Information for full images.

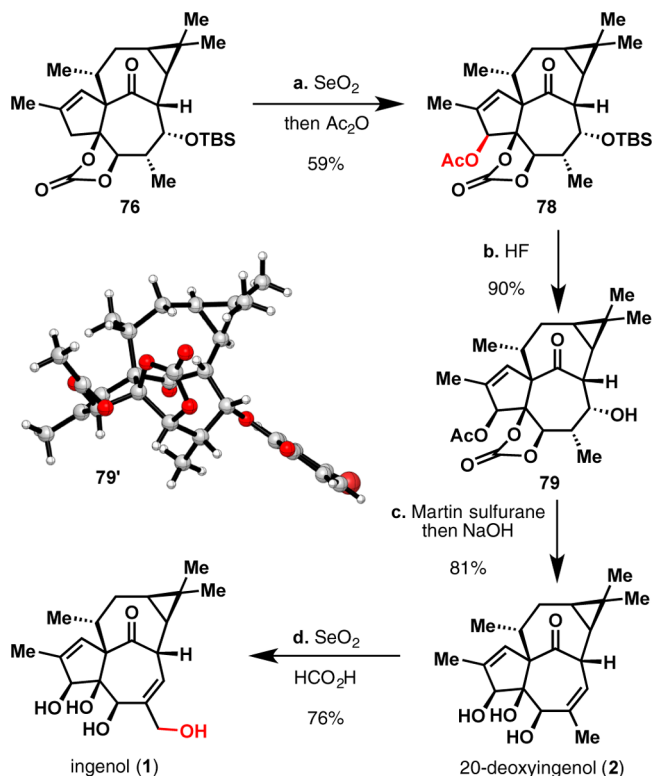
Scheme 12. Synthesis and Successful Rearrangement of Carbonate 72^a

^aReagents and conditions: (a) CDI, DMAP, CH_2Cl_2 , rt, 64% from 59; (b) MsCl, Et_3N , CH_2Cl_2 , 0°C , 77%; (c) TBAF, THF, 60°C , 45%; (d) TFA, CH_2Cl_2 , rt, 73%; (e) $\text{BF}_3 \cdot \text{Et}_2\text{O}$, CH_2Cl_2 , -78°C to -40°C , then Et_3N , MeOH , 80%; (f) HF, CH_3CN , 50°C , 89%. Abbreviations: CDI = *N,N*-carbonyldiimidazole, MsCl = methanesulfonyl chloride.

spirocyclization. Additionally, molecular modeling suggested that the orientation of the migrating bond with respect to the π -system is improved with a cyclic protecting group on the diol. Treatment of diol 66 with CDI in the presence of catalytic quantities of DMAP gives carbonate 72 in 64% yield from 59 (Scheme 12). Gratifyingly, the carbonate protecting group proved stable to acidic conditions, but submission to a variety of activating conditions produced only elimination or no reaction. Diene 73 was obtained in 77% yield by treatment of 72 with MsCl and Et_3N . To probe whether the bulky silyl protecting groups were preventing reactivity, 72 was deprotected with TBAF to provide triol 74 in 45% yield. Treatment of 74 with TFA instead produced bicyclic ether 75 in 73% yield. Extensive screening of various Lewis acids, protic acids, and activating agents on 66, 72, and 74 was unsuccessful. However, experimenting with the quenching conditions yielded very promising results. When 72 was treated with $\text{BF}_3 \cdot \text{Et}_2\text{O}$ in CH_2Cl_2 and quenched at -78°C , only starting material was recovered. When the reaction was instead warmed to 0°C , a mixture of eliminated byproducts was obtained. When the reaction was quenched with saturated aqueous NaHCO_3 at -78°C , however, a low yield of the desired product 76 was obtained. A thorough examination revealed that the temperature of the reaction quench was essential to generating the desired product, with 80% yield of 76 obtained when the reaction was quenched with 1:1 $\text{MeOH}/\text{Et}_3\text{N}$ at -40°C . While a comprehensive investigation of Lewis acids under these specific conditions has not been undertaken, successful pinacol rearrangement to product 76 has only been observed with the use of $\text{BF}_3 \cdot \text{Et}_2\text{O}$. Further experiments also illustrated that 76 is a kinetic product of the reaction. Treatment of 76 with $\text{BF}_3 \cdot \text{Et}_2\text{O}$ at 0°C produced retro-pinacol rearrangement to 77, while treatment with aqueous HF produced previously observed ether 75. Success in this instance ultimately hinged on the recognition that the vinylogous pinacol rearrangement is reversible, and so the desired, less stable product must be trapped out as a kinetic product. Further mechanistic analysis is provided below through DFT calculations.

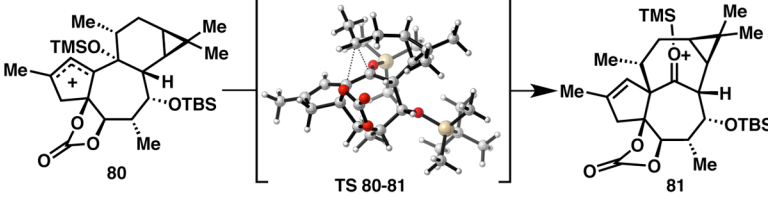
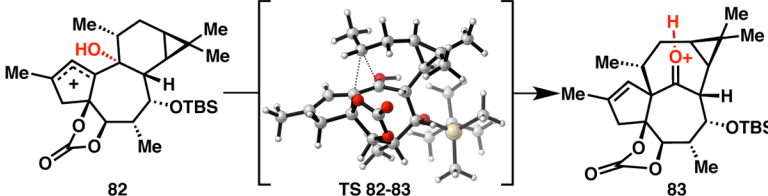
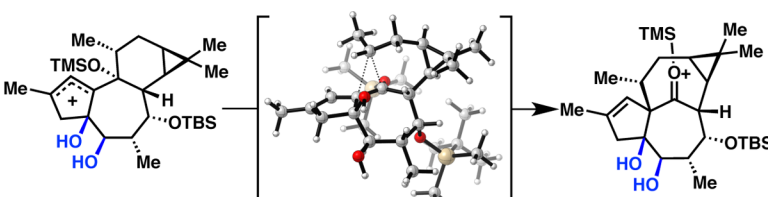
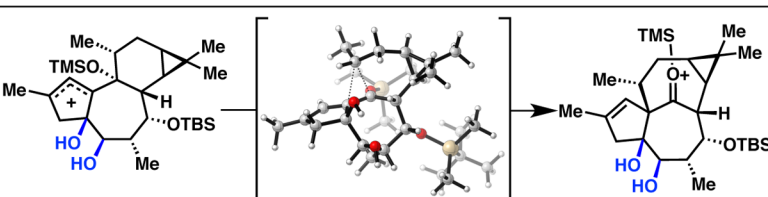
With the *in/out* bicyclic framework secured, completing the synthesis required two allylic oxidations and elimination of the TBS ether. The first allylic oxidation was accomplished with

SeO_2 , followed by *in situ* acylation with Ac_2O to provide 78 in 59% yield as a single diastereomer (Scheme 13). The observed selectivity is consistent with a previously observed preference for secondary over primary positions in SeO_2 -mediated allylic oxidation.³⁵ TBS deprotection was accomplished, without retro-pinacol rearrangement, by treatment with aqueous HF to give 79 in 90% yield. X-ray crystallographic analysis of the

Scheme 13. Completing the Total Synthesis of Ingenol (1)^a

^aReagents and conditions: (a) SeO_2 , dioxane, 80°C , then Ac_2O , DMAP, rt, 59%; (b) HF, CH_3CN , 50°C , 90%; (c) Martin sulfurane, CHCl_3 , 60°C , then 10% aq NaOH, THF, rt; (d) SeO_2 , HCO_2H , dioxane, 80°C , 76%.

Table 1. Computed Gibbs Free Energy (ΔG), Activation Energy (ΔG^\ddagger), and Relative Activation Energy ($\Delta\Delta G^\ddagger$) of Synthetic Pinacol Rearrangements^a

Reaction	ΔG	ΔG^\ddagger	$\Delta\Delta G^\ddagger$	note
	-7.0 (-4.3)	4.9 (5.1)	0	• kinetically and thermodynamically favorable
	-2.3 (1.0)	6.8 (8.0)	+1.9 (+2.9)	• silyl group reduces ΔG^\ddagger and decreases ΔG
	1.7 (2.8)	13.8 (11.6)	+8.9 (+6.5)	• carbonate protecting group lowers ΔG and reduces ΔG^\ddagger
	-3.2 (0.3)	5.0 (6.4)	+0.1 (+1.3)	• carbonate effect on ΔG^\ddagger is largely conformational • effect on ΔG is partly conformational

^aAll energies are reported in kcal/mol. Energies in **bold** are at the M06-2X/6-31+G(d,p)//B3LYP/6-31G(d) level, while energies in *italics* are at the B3LYP/6-31G(d) level. Free energies are at 298.15 K and 1 atm.

corresponding *p*-bromobenzoate **79'** established the *in/out* and acetate stereochemistry. Alcohol elimination was effected by treatment with Martin sulfurane, followed by basic work-up to remove the protecting groups, to give 20-deoxyingenol (**2**) in 81% yield. The final allylic oxidation was accomplished in a fashion analogous to the Wood synthesis.^{19c} Using Shibuya's conditions³⁶ of SeO₂ in the presence of formic acid, allylic oxidation was performed, without over-oxidation, to provide ingenol (**1**) in 76% yield. Synthetic 20-deoxyingenol (**2**) and ingenol (**1**) were spectroscopically identical to naturally obtained material. Thus, the total synthesis of ingenol was completed in 14 linear steps from (+)-3-carene to give (+)-ingenol in 1.2% overall yield (73% per step).

DFT Examination of Pinacol Rearrangement. In order to gain additional insight into the mechanism of the apparently contra-thermodynamic pinacol rearrangement, DFT calculations were performed using Gaussian 09 at the B3LYP/6-31G(d) level, with single-point energies calculated at the M06-2X/6-31+G(d,p) level (Table 1).³⁷ Initial calculations suggested that the reaction proceeds in a stepwise manner through an allylic carbocation.³⁸ When the rearrangement of carbocation **80** was examined, it was found that the reaction to form silyl oxonium **81** is both thermodynamically ($\Delta G = -7.0$ kcal/mol) and kinetically favorable ($\Delta G^\ddagger = 4.9$ kcal/mol). In order to probe the structural features that are important for

reactivity, various simplified derivatives were also examined. The rearrangement of cation **82**, lacking the TMS ether, is less thermodynamically favorable and, more importantly, requires ~ 2 kcal/mol more activation energy than **80**. More dramatically, the rearrangement of cation **84**, lacking the carbonate protecting group, is thermodynamically unfavorable ($\Delta G = 1.7$ kcal/mol) and requires ~ 9 kcal/mol additional activation energy relative to **80**. This effect appears to be predominantly conformational in nature, as the rearrangement of **84'**—in which the diol is in a conformation similar to the carbonate **80**—was nearly identical in activation energy to the rearrangement of **80**. It is ironic that the two major groups that seem to be responsible for successful reactivity, and their substantial effect on the pinacol rearrangement was unexpected.

Further mechanistic insight was gained by examining the potential energy surface (PES) for the reaction of **80** and **82**. An intrinsic reaction coordinate (IRC) calculation on **TS 80–81** reveals that the rearrangement of **80** is highly asynchronous, and the bond-breaking and bond-forming events are separated by a near plateau on the PES (Figure 2A). On the other hand, an IRC calculation on **TS 82–83** shows that, in the absence of the TMS group, the asynchronicity disappears, and the PES is only slightly flat near the transition state (Figure 2B). The same asynchronicity is observed on other compounds bearing a TMS

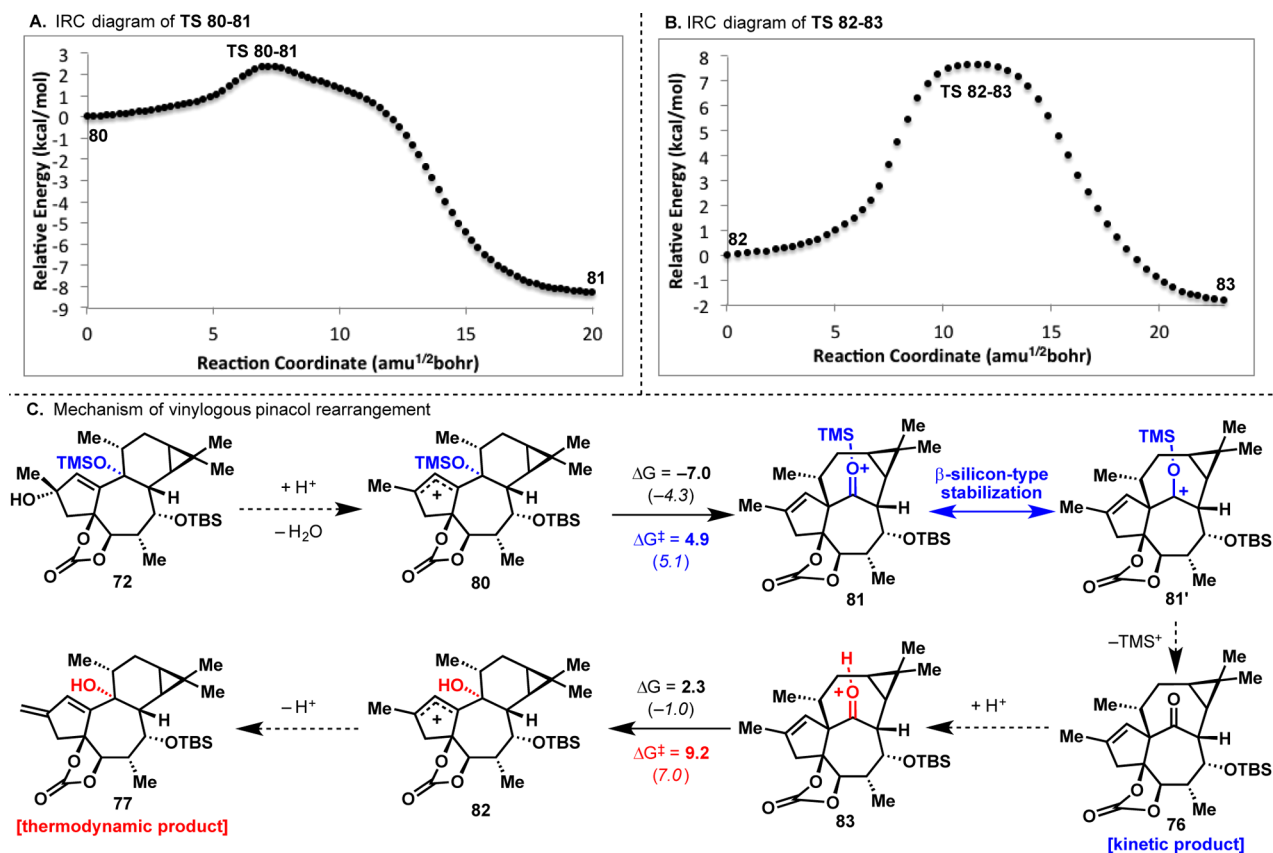


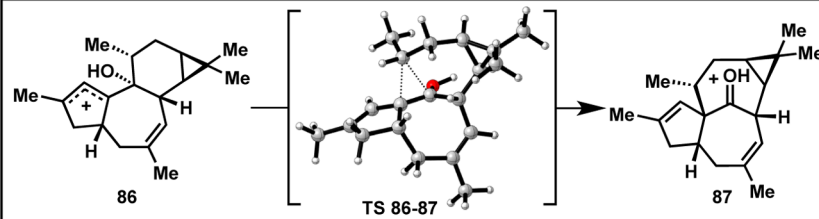
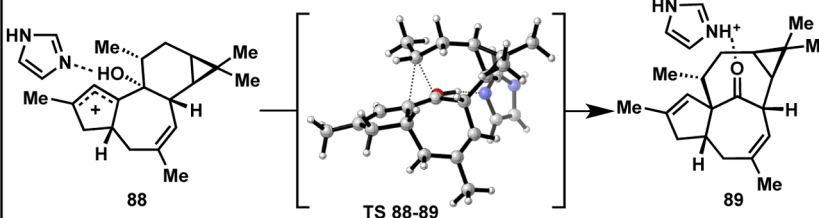
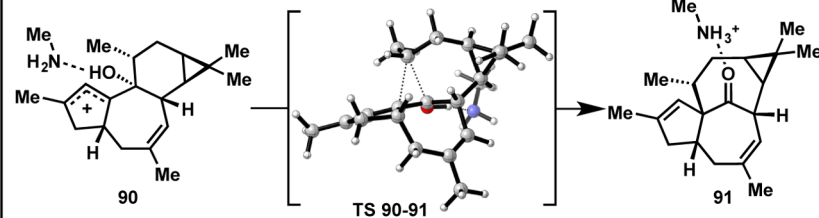
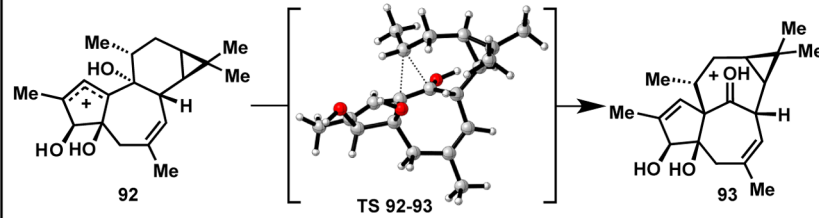
Figure 2. Mechanistic analysis of the pinacol rearrangement. (A) Intrinsic reaction coordinate (IRC) diagram of the rearrangement of 80 to 81 (energies uncorrected for ZPE). (B) IRC diagram for the rearrangement of 82 to 83 (energies uncorrected for ZPE). (C) Simplified mechanism of the vinylogous pinacol rearrangement. Energies are given in kcal/mol, and the reaction coordinate is in units of amu^{1/2}bohr. Energies in bold are at the M06-2X/6-31+G(d,p)//B3LYP/6-31G(d) level, while energies in italics are at the B3LYP/6-31G(d) level. Free energies are at 298.15 K and 1 atm. Reactions indicated by dashed arrows were not examined computationally.

group and not found on those without one.³⁹ This mechanistic shift is attributed to a stabilizing effect of the silicon atom on the positive charge in **81** and the developing positive charge in the transition state. The stabilizing effect seen here is akin to the commonly encountered β -silicon effect, exemplified by resonance structure **81'**.⁴⁰ An analogous mechanism mediated by a proton (H⁺) is shown in Figure 2C. Initial loss of water produces carbocation **80**, which rearranges exergonically to **81** over a low barrier. Loss of a TMS group—possibly in the form of TMSF in the case of BF₃·Et₂O—leads to **76** as the initially formed kinetic product. Retro-pinacol rearrangement is initiated by protonation of the ketone to form **83**. The barrier for the reverse rearrangement from **83** to **82** is predicted to be ~4 kcal/mol higher than the barrier for **80** to **81**. Thus, products **73** and **75** only arise under thermodynamic conditions when sufficient energy is available to cross the higher barrier for retro-pinacol rearrangement in the absence of the silyl group. This mechanistic picture is greatly simplified—relying on a proton instead of BF₃ and neglecting solvent effects—but it provides an approximate explanation of the factors governing the selectivity observed in the pivotal pinacol rearrangement.

Pinacol Rearrangement in the Biosynthesis of Ingenol (1). With an approximate picture of the mechanism of the pinacol rearrangement in our synthesis, we sought to expand the DFT calculations to reactions with relevance to the biosynthesis of ingenol (**1**). The simplest putative precursor of ingenol is **86**, which is an oxidized tigliane derivative with the requisite tertiary alcohol and allylic carbocation (Table 2).

Surprisingly, the rearrangement of **86** to **87** is highly endergonic ($\Delta G = 12.6$ kcal/mol), and the activation barrier is relatively high ($\Delta G^{\ddagger} = 17.8$ kcal/mol). This exemplifies the substantial strain of the ingenane ring system. The unfavorable energetics of the pinacol rearrangement must be overcome in order for the *in/out* bicycle to form in nature. Given that substituents on the tertiary alcohol seem to have a beneficial effect on the pinacol rearrangement in our synthesis, it was hypothesized that Lewis base activation of the tertiary alcohol would stabilize the transition state and reduce the activation energy. To this end, coordination of a simple imidazole or methylamine theozyme to the tertiary alcohol was found to reduce the activation energy of the pinacol rearrangement by ~5 kcal/mol.⁴¹ These results suggest that a viable mechanism for enzyme catalysis is a Lewis-basic active site amino acid (histidine or lysine), which would coordinate the tertiary alcohol and stabilize the developing positive charge in the transition state. Additionally, it is possible that additional peripheral oxidation is present in the precursor tigliane molecule prior to the pinacol rearrangement. Indeed, oxidation in the A-ring significantly reduces the activation barrier for pinacol rearrangement and destabilizes the carbocation precursor. Carbocation **92** has a ~8 kcal/mol lower energy barrier to rearrangement than **86**. This result is also consistent with observed reactivity. Compound **76** undergoes retro-pinacol rearrangement upon treatment with aqueous HF, while **78**—which has only an additional acetate on the A-ring—deprotects cleanly without rearrangement under identical

Table 2. Computed Gibbs Free Energy (ΔG), Activation Energy (ΔG^\ddagger), and Relative Activation Energy ($\Delta\Delta G^\ddagger$) of Biosynthetic Pinacol Rearrangements^a

Reaction	ΔG	ΔG^\ddagger	$\Delta\Delta G^\ddagger$	note
	12.6 (15.1)	17.8 (18.2)	0	<ul style="list-style-type: none"> kinetically and thermodynamically unfavorable
	-7.6 (-7.0)	12.8 (11.7)	-5.0 (-6.5)	<ul style="list-style-type: none"> imidazole (His) reduces activation energy potential enzyme catalysis
	-7.0 (-5.1)	12.9 (11.4)	-4.9 (-6.8)	<ul style="list-style-type: none"> amine (Lys) reduces activation energy potential enzyme catalysis
	2.9 (6.9)	9.6 (10.5)	-8.2 (-7.7)	<ul style="list-style-type: none"> A-ring oxidation reduces activation barrier post-oxidase pinacol rearrangement

^aAll energies are reported in kcal/mol. Energies in **bold** are at the M06-2X/6-31+G(d,p)//B3LYP/6-31G(d) level, while energies in *italics* are at the B3LYP/6-31G(d) level. Free energies are at 298.15 K and 1 atm.

conditions. These results suggest that electron-withdrawing substituents around the allylic carbocation destabilize the tigliane precursor relative to the rearrangement product, so a pinacol rearrangement after peripheral p450 oxidation would be more favorable. Overall, two distinct mechanisms have been proposed that could act synergistically to render the biosynthetic pinacol rearrangement more kinetically and thermodynamically favorable.

CONCLUSION

Ingenol (**1**) has tested the creativity of synthetic chemists for nearly three decades with its unique architecture and stereochemical challenge. It is a fabulous case study for a terpene that attracted enormous attention initially based solely on its challenging structural features and later because of its proven medicinal properties. Those path-pointing studies, outlined in dozens of research articles and theses, formed a solid foundation for the development of a concise synthesis of (+)-ingenol (**1**), as outlined in this full account. Armed with a retrosynthesis featuring a biomimetic yet speculative pinacol rearrangement, we developed a two-phase approach featuring an allene-yne P-K reaction to establish a tigliane-type precursor in only 7 steps. Competitive rearrangements were tamed in

order to discover a kinetically controlled, vinylogous pinacol rearrangement that furnishes the *in/out* bicyclic core in a further 3 steps. The oxidase phase was completed through the use of stereo- and regioselective allylic oxidations to deliver (+)-ingenol (**1**) in only 14 steps from (+)-3-carene (**36**). The high level of redox economy is an especially notable feature of the synthesis; however, of the 14 steps, 5 are concession steps, and thus even further refinement to this route can be envisioned.⁴² In addition to providing a concise route to **1**, the synthesis adds validity to the biosynthetic proposal of a pinacol rearrangement to form the *in/out* bicyclic skeleton of **1**. Finally, DFT calculations were employed to further understand factors influencing the pinacol rearrangement in the context of both the chemical synthesis and the biosynthesis of **1**. The synthesis of ingenol (**1**) presented herein allows access to novel, fully synthetic analogues of the anti-cancer drug ingenol mebutate (Picato, **3**) and provides a blueprint for commercial production. Further work on improving the scalability of the synthesis and the preparation of new analogues of **3** is ongoing in collaboration with LEO Pharma and will be reported in due course.

■ ASSOCIATED CONTENT

■ Supporting Information

Experimental details, spectra, X-ray crystallographic data, computational details, and computed structures and energies. This material is available free of charge via the Internet at <http://pubs.acs.org>.

■ AUTHOR INFORMATION

Corresponding Author

pbaran@scripps.edu

Author Contributions

[†]L.J. and C.A.K. contributed equally to this work.

Notes

The authors declare no competing financial interest.

■ ACKNOWLEDGMENTS

Financial support for this work was provided by LEO Pharma. The Carlsberg Foundation and Danish Council for Independent Research (Technology and Production Sciences) provided postdoctoral fellowships for L.J., and the Alexander von Humboldt Foundation provided a postdoctoral fellowship for C.A.K. We are grateful to J. Felding and H. Bladh (LEO Pharma) for generous discussions. We thank LEO Pharma for generous donations of natural samples of ingenol and 20-deoxyingenol and the High-Performance Computing Center (TSRI) for computational services. We thank Prof. A Rheingold and C. Moore (UCSD) for X-ray crystallographic measurements and G. Siuzdak (TSRI) for mass spectrometry assistance. A provisional patent application has been filed and is available under patent application no. U.S. 61/829,861.

■ REFERENCES

- (1) Maimone, T. J.; Baran, P. S. *Nat. Chem. Biol.* **2007**, *3*, 396–407.
- (2) (a) Velluz, L.; Valls, J.; Nominé, G. *Angew. Chem., Int. Ed.* **1965**, *41*, 181–200. (b) Yoder, R. A.; Johnston, J. N. *Chem. Rev.* **2005**, *105*, 4730–4756.
- (3) (a) Corey, E. J.; Ohno, M.; Vatakencherry, P. A.; Mitra, R. B. *J. Am. Chem. Soc.* **1961**, *83*, 1251–1253. (b) Corey, E. J.; Ohno, M.; Mitra, R. B.; Vatakencherry, P. A. *J. Am. Chem. Soc.* **1964**, *86*, 478–485. (c) Corey, E. J.; Cheng, X. *The Logic of Chemical Synthesis*; John Wiley & Sons: New York, 1995.
- (4) (a) Rapson, W. S.; Robinson, R. *J. Chem. Soc.* **1935**, 1285–1288. (b) Lo, J. C.; Yabe, Y.; Baran, P. S. *J. Am. Chem. Soc.* **2014**, *136*, 1304–1307. (c) McCarroll, A. J.; Walton, J. C. *Angew. Chem., Int. Ed.* **2001**, *40*, 2224–2248.
- (5) (a) Raskin, I.; Ribnick, D. M.; Komarnytsky, S.; Ilic, N.; Poulev, A.; Borisjuk, N.; Brinker, A.; Moreno, D. A.; Ripoll, C.; Yakoby, N.; O'Neal, J. M.; Cornwell, T.; Pastor, I.; Fridlender, B. *Trends in Biotechnol.* **2002**, *20*, 522–531. (b) Koehn, F. E.; Carter, G. T. *Nat. Rev. Drug Discov.* **2005**, *4*, 206–220. (c) Yang, H.; Dou, Q. P. *Curr. Drug Targets* **2010**, *11*, 733–744. (d) Gershenzon, J.; Dudareva, N. *Nat. Chem. Biol.* **2007**, *3*, 408–414.
- (6) (a) Jorgensen, L.; McKerrall, S. J.; Kutruff, C. A.; Ungeheuer, F.; Felding, J.; Baran, P. S. *Science* **2013**, *341*, 878–882. (b) Appendino, G. *Angew. Chem., Int. Ed.* **2014**, *53*, 927–929.
- (7) Hecker, E. *Pure Appl. Chem.* **1977**, *49*, 1423–1431.
- (8) Hecker, E. *Cancer Res.* **1968**, *28*, 2338–2348.
- (9) Zeichmeister, K.; Brandl, F.; Hoppe, W.; Hecker, E.; Opferkuch, H. J.; Adolf, W. *Tetrahedron Lett.* **1970**, *47*, 4075–4078.
- (10) Only one additional natural product type is known to contain *in/out* stereochemistry, and it contains a macrocyclic (14-membered) ring in the bicycle skeleton. See ref 11.
- (11) For a review of *in/out* isomerism, see: Alder, R. W.; East, S. P. *Chem. Rev.* **1996**, *96*, 2097–2111.
- (12) (a) Ogbourne, S. M.; Suhrbier, A.; Jones, B.; Cozzi, S.; Boyle, G. M.; Morris, M.; McAlpine, D.; Johns, J.; Scott, T. M.; Sutherland, K. P.; Gardner, J. M.; Le, T. T. T.; Lenarczyk, A.; Aylward, J. H.; Parsons, P. G. *Cancer Res.* **2004**, *64*, 2833–2839. (b) Fujiwara, M.; Fujiwara, M.; Ijichi, K.; Tokuhisa, K.; Katsuura, K.; Shigetani, S.; Konno, K.; Wang, G. Y.; Uemura, D.; T Yokota, T.; Baba, M. *Antimicrob. Agents Chemother.* **1996**, *40*, 271–273.
- (13) U.S. Food and Drug Administration, 2012 Novel New Drugs Summary (FDA, Washington, DC, 2013); www.fda.gov/downloads/Drugs/DevelopmentApprovalProcess/DrugInnovation/UCM337830.pdf.
- (14) For a review of the development of ingenol mebutate (3), see: Vasas, A.; Rédei, D.; Csupor, D.; Molnár, J.; Hohmann, J. *Eur. J. Org. Chem.* **2012**, 5115–5130.
- (15) (a) Siller, G.; Rosen, R.; Freeman, M.; Welburn, P.; Katsamas, J.; Ogbourne, S. M. *Aust. J. Dermatol.* **2010**, *51*, 99–105. (b) ClinicalTrials.gov, NCT00329121, <http://clinicaltrials.gov/show/NCT00329121>.
- (16) (a) Rosen, R. H.; Gupta, A. K.; Tying, S. K. *J. Am. Acad. Dermatol.* **2012**, *66*, 486–493. (b) Ersvaer, E.; Kittang, A. O.; Hampson, P.; Sand, K.; Gjertsen, B. T.; Lord, J. M.; Bruserud, Ø. *Toxins* **2010**, *2*, 174–194. (c) Serova, M.; Ghoul, A.; Benhadji, K. A.; Faivre, S.; Le Tourneau, C.; Cvitkovic, E.; Lokiec, F.; Lord, J.; Ogbourne, S. M.; Calvo, F.; Raymond, E. *Mol. Cancer Ther.* **2008**, *7*, 915–922.
- (17) Hohmann, J.; Evanics, F.; Berta, L.; Bartók, T. *Planta Med.* **2000**, *66*, 291–294.
- (18) (a) Liang, X.; Grue-Sørensen, G.; Petersen, A. K.; Högberg, T. *Synlett* **2012**, 23, 2647–2652. (b) Appendino, G.; Tron, G. C.; Cravatto, G.; Palmisano, G.; Jakupovic, J. *Nat. Prod. Rep.* **1999**, *62*, 76–79.
- (19) (a) Winkler, J. D.; Rouse, M. B.; Greaney, M. F.; Harrison, S. J.; Jeon, Y. T. *J. Am. Chem. Soc.* **2002**, *124*, 9726–9728. (b) Tanino, K.; Onuki, K.; Asano, K.; Miyashita, M.; Nakamura, T.; Takahashi, Y.; Kuwajima, I. *J. Am. Chem. Soc.* **2003**, *125*, 1498–1500. (c) Nickel, A.; Maruyama, T.; Tang, H.; Murphy, P. D.; Greene, B.; Yusuff, N.; Wood, J. L. *J. Am. Chem. Soc.* **2004**, *126*, 16300–16301.
- (20) Ohyoshi, T.; Ohyoshi, T.; Funakubo, S.; Miyazawa, Y.; Niida, K.; Hayakawa, I.; Kigoshi, H. *Angew. Chem., Int. Ed.* **2012**, *51*, 4972–4975.
- (21) For thorough reviews of the approaches to and syntheses of ingenol, see: (a) Kim, S.; Winkler, J. D. *Chem. Soc. Rev.* **1997**, *26*, 387–399. (b) Kuwajima, I.; Tanino, K. *Chem. Rev.* **2005**, *105*, 4661–4670. (c) Cha, J. K.; Epstein, O. L. *Tetrahedron* **2006**, *62*, 1329–1343.
- (22) (a) Kutruff, C. A.; Eastgate, M. D.; Baran, P. S. *Nat. Prod. Rep.* **2014**, *31*, 419–432. (b) Szpilman, A. M.; Carreira, E. M. *Angew. Chem., Int. Ed.* **2010**, *49*, 9592–9628. (c) Newhouse, T.; Baran, P. S.; Hoffmann, R. W. *Chem. Soc. Rev.* **2009**, *38*, 3010–3021. (d) Wender, P. A.; Verma, V. A.; Paxton, T. J.; Pillow, T. H. *Acc. Chem. Res.* **2008**, *41*, 40–49.
- (23) (a) Adolf, W.; Hecker, E. *Isr. J. Chem.* **1977**, *16*, 75–83. (b) Schmidt, R. J. *Bot. J. Linn. Soc.* **1987**, *94*, 221–230.
- (24) Kirby, J.; Nishimoto, M.; Park, J. G.; Withers, S. T.; Nowroozi, F.; Behrendt, D.; Garcia Rutledge, E. J.; Fortman, J. L.; Johnson, H. E.; Anderson, J. V.; Keasling, J. D. *Phytochemistry* **2010**, *71*, 1466–1473.
- (25) Appendino, G.; Tron, G. C.; Cravotto, G.; Palmisano, G.; Annunziata, R.; Baj, G.; Surico, N. *Eur. J. Org. Chem.* **1999**, 3413–3420.
- (26) Epstein, O. L.; Cha, J. K. *Angew. Chem., Int. Ed.* **2005**, *44*, 121–123.
- (27) (a) Paquette, L. A.; Zhao, Z.; Gallou, F.; Liu, J. *J. Am. Chem. Soc.* **2000**, *122*, 1540–1541. (b) Paquette, L. A.; Gallou, F.; Zhao, Z.; Young, D. G.; Liu, J.; Yang, J.; Friedrich, D. *J. Am. Chem. Soc.* **2000**, *122*, 9610–9620.
- (28) (a) Ishihara, Y.; Baran, P. S. *Synlett* **2010**, 12, 1733–1745. (b) Chen, K.; Baran, P. S. *Nature* **2009**, *459*, 824–828. (c) Mendoza, A.; Ishihara, Y.; Baran, P. S. *Nat. Chem.* **2012**, *4*, 21–25. (d) Chorney, E. C.; Green, J. C.; Baran, P. S. *Angew. Chem., Int. Ed.* **2013**, *52*, 9019–9022.

(29) (a) Blanco-Urgoiti, J.; Añorbe, L.; Pérez-Serrano, L.; Domínguez, G.; Pérez-Castells, J. *Chem. Soc. Rev.* **2004**, *33*, 32–42. (b) Shibata, T. *Adv. Synth. Catal.* **2006**, *348*, 2328–2336. For an example of a Pauson–Khand reaction in a scalable total synthesis, see: (c) Su, S.; Rodriguez, R. A.; Baran, P. S. *J. Am. Chem. Soc.* **2011**, *133*, 13922–13925.

(30) At the time of writing, (+)-3-carene (90% chemical purity) is commercially available from Sigma-Aldrich for \$86/L (115576-1L).

(31) The requisite methyl ketone (SI-6) has a noteworthy history. The enantiomer was examined (as a mixture of diastereomers) in 1967 by H. C. Brown and A. Suzuki, who surprisingly found it is the thermodynamically disfavored diastereomer: (a) Brown, H. C.; Suzuki, A. *J. Am. Chem. Soc.* **1967**, *89*, 1933–1941. Later, Paquette and co-workers attempted to synthesize SI-6 for use in phorbol (23) and ingenol (1) total syntheses but were unable to form it with acceptable regio- or stereocontrol. These struggles are detailed at length in the following and were very inspirational to our work: (b) Paquette, L. A.; Ross, R. J.; Shi, Y. *J. Org. Chem.* **1990**, *55*, 1589–1598. We examined several different approaches before success was achieved as described.

(32) Lovely, C. J.; Seshadri, H.; Wayland, B. R.; Cordes, A. W. *Org. Lett.* **2001**, *3*, 2607–2610.

(33) (a) Mukai, C.; Nomura, I.; Yamanishi, K.; Hanaoka, M. *Org. Lett.* **2002**, *4*, 1755–1758. (b) Brummond, K. M.; Chen, H.; Fisher, K. D.; Kerekes, A. D.; Rickards, B.; Sill, P. C.; Geib, S. J. *Org. Lett.* **2002**, *4*, 1931–1934. (c) Mukai, C.; Nomura, I.; Kitagaki, S. *J. Org. Chem.* **2003**, *68*, 1376–1385. (d) Brummond, K. M.; Chen, D.; Davis, M. M. *J. Org. Chem.* **2008**, *73*, 5064–5068.

(34) For a mechanistic study on over-oxidation in OsO₄-catalyzed dihydroxylations, see: Lohray, B. B.; Bhushan, V.; Kumar, R. K. *J. Org. Chem.* **1994**, *59*, 1375–1380.

(35) (a) Hoekstra, W. J.; Fairlamb, I. J. S.; Giroux, S. *Selenium(IV) Oxide. e-EROS Encyclopedia of Reagents for Organic Synthesis*; John Wiley & Sons, Ltd.: New York, 2007 (DOI: 10.1002/047084289X.rs008.pub2). (b) Nakamura, A.; Nakata, M. *Synthesis* **2013**, *45*, 1421–1451.

(36) Shibuya, K. *Synth. Commun.* **1994**, *24*, 2923–2941.

(37) (a) Becke, A. D. *J. Chem. Phys.* **1993**, *98*, 5648–5652. (b) Zhao, Y.; Truhlar, D. G. *Theor. Chem. Acc.* **2008**, *120*, 215–241. Gaussian 09 was utilized for all calculations: (c) Frisch, M. J.; et al. *Gaussian09*, Revision D.01; Gaussian, Inc.: Pittsburgh, PA, 2009 (full reference in the Supporting Information). ; Structures were visualized with CYLView: (d) Legault, C. Y. *CYLview*, 1.0b; Université de Sherbrooke: Quebec, Canada, 2009; <http://www.cylview.org>. A detailed procedure for calculations and a full list of references for computational methods employed is provided in the Supporting Information. Computed energies at the mPW1PW91/6-31+G(d,p)//B3LYP/6-31G(d) level and additional computed structures and energies relevant to the biosynthesis of **1** are also presented in the Supporting Information.

(38) Protonated **72** was not found to be a stationary point. Instead, geometry optimization of protonated **72** led to carbocation **80** and H₂O, indicating the activation barrier for ionization is very low or zero and the reaction downhill in energy. Additionally, in a related compound series, both epimers of the tertiary alcohol provide product, implying a cationic mechanism.

(39) Additional support for an asynchronous reaction can be found in the plot of RMS gradient along the IRC (see Supporting Information).

(40) Wierschke, S. G.; Chandrasekhar, J.; Jorgensen, W. L. *J. Am. Chem. Soc.* **1985**, *107*, 1496–1500.

(41) For a review on the use of theozymes (theoretical enzyme mimics made up of model functional groups) in computational chemistry, see: Tantillo, D. J.; Chen, J.; Houk, K. N. *Curr. Opin. Chem. Biol.* **1998**, *2*, 743–750.

(42) For detailed discussions of redox economy and step economy, see: (a) Burns, N. Z.; Baran, P. S.; Hoffmann, R. W. *Angew. Chem., Int. Ed.* **2009**, *48*, 2854–2867. (b) Gaich, T.; Baran, P. S. *J. Org. Chem.* **2010**, *75*, 4657–4673.

■ NOTE ADDED AFTER ASAP PUBLICATION

The structures for compounds **29** and **30** in Scheme 3 were corrected, and the reagents used to give diol **39** were corrected in the text discussion of Scheme 5. The corrected version was re-posted on April 16, 2014.